Acyl-CoA-binding protein, Acb1p, is required for normal vacuole function and ceramide synthesis in *Saccharomyces cerevisiae*

Nils J. FÆRGEMAN*, Søren FEDDERSEN*, Janne K. CHRISTIANSEN*, Morten K. LARSEN*, Roger SCHNEITER†, Christian UNGERMANN‡, Kudzai MUTENDA*, Peter ROEPSTORFF* and Jens KNUDSEN*[1]

*Department of Biochemistry and Molecular Biology, University of Southern Denmark, Campusvej 55, DK-5230 Odense M, Denmark, †Division of Biochemistry, Department of Medicine, University of Fribourg. Chemin du Musée 5, CH 1700 Fribourg, Switzerland, and ‡Biochemie-Zentrum Heidelberg, Im Neuenheimer Feld 328, 3. OG, D-69120, Heidelberg, Germany

In the present study, we show that depletion of acyl-CoA-binding protein, Acb1p, in yeast affects ceramide levels, protein trafficking, vacuole fusion and structure. Vacuoles in Acb1p-depleted cells are multi-lobed, contain significantly less of the SNAREs (soluble *N*-ethylmaleimide-sensitive fusion protein attachment protein receptors) Nyv1p, Vam3p and Vti1p, and are unable to fuse *in vitro*. Mass spectrometric analysis revealed a dramatic reduction in the content of ceramides in whole-cell lipids and in vacuoles isolated from Acb1p-depleted cells. Maturation of yeast aminopeptidase I and carboxypeptidase Y is slightly delayed in Acb1p-depleted cells, whereas the maturation of alkaline phosphatase and Gas1p is unaffected. The fact that Gas1p maturation is unaffected by Acb1p depletion, despite the lowered ceramide content in these cells, indicates that ceramide synthesis in yeast could be compartmentalized. We suggest that the reduced ceramide synthesis in Acb1p-depleted cells leads to severely altered vacuole morphology, perturbed vacuole assembly and strong inhibition of homotypic vacuole fusion.

Key words: acyl-CoA-binding protein (ACBP), ceramide, electrospray ionization mass spectrometry (ESI–MS), membrane fusion, soluble *N*-ethylmaleimide-sensitive fusion protein attachment protein receptor (SNARE), vacuole.

INTRODUCTION

The maintenance and physiological integrity of distinct cellular compartments relies on highly selective protein and lipid trafficking pathways. Neither vesicle formation, termed membrane fission, nor vesicle fusion is completely understood. However, the establishment of *in vitro* fission and fusion assays has increased our insights into the molecular mechanisms of how these processes are regulated [1]. Most of this work has focused on identifying proteins required for these processes and to uncover their function. Little is known about the lipid requirement; however, over the last few years, it has been shown that the lipid composition of the membrane bilayer is important, and that lipids serve as important players in vesicular trafficking [2,3]. A role for sphingolipids in endocytosis and in vesicular transport of GPI (glycosylphosphatidylinositol)-anchored proteins out of the ER (endoplasmic reticulum) is supported by several studies (see [4] for a review). Long-chain bases (LCBs), independent of their conversion into ceramide or LCB-phosphates, have been shown to play a critical role in the regulation of endocytosis. Ceramide/sphingolipid synthesis in the ER is required for efficient transport of GPI-anchored proteins from ER to Golgi, and recent *in vitro* experiments also suggest a function of these lipids in the fusion of vesicles containing GPI-anchored proteins with the Golgi [5].

It is well known that long-chain (C_{14}–C_{18}) fatty acyl-CoA esters can serve as important cofactors in budding, as well as fusion of transport vesicles (reviewed in [6]). Haas and Wickner [7] observed that myristoyl-, palmitoyl-CoA and CoASH, in contrast with short- and very-long-chain acyl-CoA esters, support vacuole fusion *in vitro*. Interestingly, non-hydrolysable long-chain acyl-CoA ester analogue inhibited homotypic vacuole fusion [7], as well as Golgi fusion and fission [8–10]. This indicates that the acyl-CoA ester acts as substrate in a protein or lipid acylation. Interestingly, a vacuolar fusion protein Vac8p is both myristoylated and palmitoylated [11,12]. Moreover, the fission catalyst CtBP/BARS (C-terminal-binding protein/brefeldin A-ADP ribosylated substrate) at the Golgi, and endophilin at the plasma membrane, catalyse the formation of phosphatidic acid from lysophosphatidic acid and acyl-CoA [13,14].

Acyl-CoA binding protein (ACBP) is a highly conserved 10 kDa protein found in all eukaryotes [15]. ACBP belongs to a multigene family comprising four major subfamilies. The basic isoform is highly conserved, and is found in all eukaryotic species examined, ranging from yeast and plants to reptiles, birds and mammals [16]. ACBP binds specifically long-chain acyl-CoA esters with an affinity of approx. 1 nM [17]. The majority of the cellular long-chain acyl-CoA esters is therefore presumed to be sequestered by ACBP *in vivo* (reviewed in [17]). The ability of ACBP to mediate intermembrane acyl-CoA transport *in vitro* [18] and to create an intracellular acyl-CoA pool [19] indicates that ACBP is involved in intracellular trafficking of acyl-CoA esters. Depletion of Acb1p in *Saccharomyces cerevisiae* results in reduced levels of very-long-chain fatty acids (C_{26}), sphingolipid synthesis, membrane assembly and organization and organelle structures [20]. These observations suggest that Acb1p may be directly or indirectly involved in vesicular trafficking and in the maintenance of the integrity of cellular compartments.

In the present study, we have investigated the effect of depleting the *S. cerevisiae* ACBP homologue Acb1p on vesicular protein trafficking, vacuole structure and fusion, and on the overall lipid

Abbreviations used: ACBP, acyl-CoA-binding protein; ALP, alkaline phosphatase; API, aminopeptidase I; CPY, carboxypeptidase Y; DHS, dehydrosphingosine; ER, endoplasmic reticulum; ESI–MS, electrospray ionization mass spectrometry; GFP, green fluorescent protein; GPI, glycosylphosphatidylinositol; IPC, inositol-phosphoceramide; NSF, *N*-ethylmaleimide-sensitive fusion protein; PHS, phytosphingosine; PrA, proteinase A; (t/v-)SNARE, (target/vesicular) soluble *N*-ethylmaleimide-sensitive fusion protein attachment protein receptor; VLCFA, very-long-chain fatty acid; YNB, Yeast Nitrogen Base.

[1] To whom correspondence should be addressed (e-mail jkk@bmb.sdu.dk).

Table 1 Strains used in the present work

Strain	Genotype	Source or reference
Y700	*MATa, ade2-1 trp1 can1-100 leu2-3 leu2-112 his3-11 his3-15 ura3,*	[20]
Y700*pGAL-ACB1*	*MATa, ade2-1 trp1 can1-100 leu2-3 leu2-112 his3-11 his3-15 ura3, pGAL-ACB1::KanMX*	[20]
W303a-1A	*MAT**a** can1-100 ade2-1 his3-11,15 leu2-3 112 trp1-1 ura3-1*	Professor A. Conzelmann
BJ3505	*Mat**a** pep4::HIS3 prb1-Δ1.6R HIS3 lys2-208 trp1-Δ101 ura3-52 gal2 can*	[24]
BJ2168	*Mata, leu2, trp1, ura3-52, prb1-1122, pep4-3*	[51]
DKY6281	*Mat**a** leu2-3 leu2-112 ura3-53 his3-Δ200 trp1-Δ901 lys2-801 suc2-Δ9 pho8::TRP1*	[24]
K91-1A	*Matα ura3 pho8::pAL134 pho13::pH13 lys1*	[7]
Y700 *pho8Δ*	*MATa, ade2-1 trp1 can1-100 leu2-3 leu2-112 his3-11 his3-15 ura3, PHO8::URA3*	The present study
Y700*pGAL-ACB1pho8Δ*	*MATa, ade2-1 trp1 can1-100 leu2-3 leu2-112 his3-11 his3-15 ura3, pGAL-ACB1::KanMX, PHO8::URA3*	The present study
Y700 *pep4Δ*	*MATa, ade2-1 trp1 can1-100 leu2-3 leu2-112 his3-11 his3-15 ura3, PEP4::His3MX*	The present study
Y700*pGAL-ACB1pep4Δ*	*MATa, ade2-1 trp1 can1-100 leu2-3 leu2-112 his3-11 his3-15 ura3, pGAL-ACB1::KanMX, pep4::His3MX*	The present study
Y700 *Vam3^{tsf}*	*MATa, ade2-1 trp1 can1-100 leu2-3 leu2-112 his3-11 his3-15 ura3, VAM3::LEU2* pRS316-*Vam3^{tsf}*	The present study
Y700*pGAL-ACB1 Vam3^{tsf}*	*MATa, ade2-1 trp1 can1-100 leu2-3 leu2-112 his3-11 his3-15 ura3, pGAL-ACB1::KanMX,VAM3::LEU2,* pRS316-*Vam3^{tsf}*	The present study
BJ3505*pGAL-ACB1*	*Mat**a**, pep4::HIS3 prb1-Δ1.6R HIS3 lys2-208 trp1-Δ101 ura3-52 gal2 can pGAL-ACB1::KanMX*	The present study
BJ2168*pGAL-ACB1*	*Mata, leu2, trp1, ura3-52, prb1-1122, pep4-, pGAL-ACB1::KanMX*	The present study
DKY6281*pGAL-ACB1*	*Mat**a**, leu2-3 leu2-112 ura3-53 his3-Δ200 trp1-Δ901 lys2-801 suc2-Δ9 pho8::TRP1 pGAL-ACB1::KanMX*	The present study
K91-1A *pGAL-ACB1*	*Matα, ura3 pho8::pAL134 pho13::pH13 lys1*	The present study
sec18	*Mata,sec18 leu2 his3 ade2-1*	The present study
sec18 pGAL-ACB1	*Mata,sec18 leu2 his3 ade2-1 pGAL-ACB1::KanMX*	The present study
sec23	*Mata,sec23 leu2-112 his3-15 ade2-1 trp1 lys1*	The present study
sec23 pGAL-ACB1	*Mata,sec23 leu2 his3 ade2-1 trp1 lys1 pGAL-ACB1::KanMX*	The present study
Ret1-1	*Mata, ret1-1 leu2 ura3 lys1 his3,*	The present study
Ret1-1 pGAL-ACB1	*Mata, ret1-1 leu2 ura3 lys1 his3 pGAL-ACB1::KanMX*	The present study
Lag1Δlac1Δ	same as W303-1A, but *lac1Δ::LEU2 lag1ΔTRP1*	Professor A. Conzelmann
Lcb1^{ts}	*MATa end8-1 leu2 ura3 his4 bar1*	[52]

profile using ESI–MS (electrospray ionization mass spectrometry). Depletion of Acb1p results in a slightly reduced protein transport to the vacuole, severe morphological alterations of the vacuole, impairment of homotypic vacuole fusion and a dramatic reduction in the cellular content of ceramide.

MATERIALS AND METHODS

Chemicals

Bacto-peptone, yeast extract and YNB (Yeast Nitrogen Base) were purchased from Difco (Diagnostic Systems, Sparks, MD, U.S.A.). EXPRE^{35}S was obtained from NEN Life Science Products (Boston, MA, U.S.A.). Protein A beads were from Amersham Biosciences (Uppsala, Sweden). FM 4-64 and antibodies against Pep12p and Pho8p were purchased from Molecular Probes (Eugene, OR, U.S.A.). Secondary antibodies were obtained from Promega (Madison, WI, U.S.A.). All chemicals were of analytical grade.

Yeast strains, culture media and genetic manipulations

The *S. cerevisiae* strains used in the present study are shown in Table 1. YPD medium consists of 1 % yeast extract, 2 % bacto-peptone and 2 % glucose supplemented with 200 mg/l adenine. YPgal medium consists of 1 % yeast extract, 2 % bacto-peptone and 2 % galactose supplemented with 200 mg/l adenine. Unless stated otherwise, yeast strains were cultivated at 30 °C in supplemented minimal YNB medium containing 2 % glucose and the appropriate amino acid mixture and uracil. Unless otherwise stated, cells were kept on YP-galactose plates and inoculated in YNB medium supplemented with 2 % glucose to a D_{600} of 0.005. Cells were grown for 24 h, diluted into fresh medium to an D_{600} of 0.05–0.1 and grown to the D_{600} indicated. The *GAL1* promoter was inserted in front of the *ACB1* gene, as described in [20]. The open reading frames encoding Pho8p and Pep4p were deleted using one-step disruption, as described in [21]. Y700, Y700 *pGAL-ACB1*, BJ3505, BJ2168 and DKY6281 strains were rendered competent using lithium acetate, as described in [22]. Transformants were selected on YP plates supplemented with 2 % galactose and 0.2 mg/ml G418, except for BJ3505 transformants, which were selected on YP plates supplemented with 2 % galactose, 4 % sucrose and 0.2 mg/ml G418, or on selective minimal plates without uracil or histidine. The correct insertion was confirmed by both PCR analysis and Western blotting. Depletion of Acb1p was confirmed by Western blotting after each experiment.

Pulse–chase analysis, protein extraction and immunoprecipitation

Cells were grown overnight in supplemented minimal glucose media without methionine. Cells were diluted to an D_{600} of 0.05–0.1 in fresh medium without methionine, and grown to a D_{600} of 0.8. Cells (2.5×10^7 per time point) were pulsed with 200 μCi of ^{35}S-protein-labelling mix (EXPRE^{35}S) for 5 min at 30 °C, and then chased with 0.1 mg/ml methionine and 0.1 mg/ml cysteine. For temperature-sensitive strains, cells were grown in selective, supplemented minimal glucose media overnight at 26 °C, diluted in fresh media without cysteine and methionine and grown to a D_{600} of 1. Cells were then divided into two equal portions, and placed at 26 °C and at 38 °C, respectively. After 15 min, cells were pulse-labelled for 10 min. At the time indicated, cell metabolism was stopped by the addition of 20 mM NaN_3 and 20 mM NaF, and the cells were placed on ice. Cells were then harvested by centrifugation and lysed using glass beads in 200 μl of ice-cold 50 mM Tris/HCl, pH 7.5, containing 5 mM EDTA and protease inhibitors (Complete™ EDTA-free; Roche). SDS was added to a final concentration of 0.5 %, and extracts were boiled for 5 min. Immunoprecipitation buffer [20 mM Tris/HCl (pH 7.5)/120 mM NaCl/5 mM EDTA/1 % (v/v) Triton X-100] was added to a total volume of 1 ml, and samples were centrifuged at 15000 ***g*** for 10 min at 4 °C. The pellet was re-extracted with

immunoprecipitation buffer, and the two supernatants were combined and transferred to a 15 ml Falcon tube containing 4 ml of immunoprecipitation buffer. Antiserum and Protein A beads (Amersham Biosciences) were added, and the suspension was incubated end-over-end overnight at 4 °C. Beads were washed several times with immunoprecipitation buffer, and proteins were eluted by boiling beads in SDS/PAGE sample buffer for 5 min and subjected to SDS/PAGE and fluorography.

Protein extraction, electrophoresis and Western blotting

Cells (1 D_{600} unit) were pelleted by centrifugation and resuspended in 0.2 M NaOH. After 15 min incubation on ice, trichloroacetic acid was added to a concentration of 10 % (w/v), and then placed on ice for 15 min. Precipitated proteins were recovered by centrifugation for 15 min at 12000 ***g*** at 4 °C. Precipitates were washed with ice-cold acetone, dried and dissolved in SDS-sample buffer. Whole-cell extracts (1D_{600} unit) and vacuolar proteins (1 μg) were separated by SDS/PAGE, transferred to a nitrocellulose membrane, and specific proteins were identified by Western blotting using enhanced chemiluminescence, as described by the manufacturer (Amersham Biosciences). Antiserum towards Tlg2p was provided by Professor Susan Ferro-Novick (Department of Cell Biology, Yale University of Medicine, CT, U.S.A.), Vac8p was either provided by Professor Lois Weisman (Department of Biochemistry, University of Iowa, IA, U.S.A.) or prepared as described in [23], API (aminopeptidase I) was either provided by Professor Daniel Klionsky (Department of Biology, University of Michigan, MI, U.S.A.) or was obtained by immunizing rabbits with purified recombinant API, CPY (carboxypeptidase Y) was from Dr Jakob Winther (Carlsberg Laboratory, Copenhagen, Denmark), Kex2p was from Ivan Dierz (Novo-Nordisk A/S, Bagsvaerd, Denmark), Gas1p was from Professor Andreas Conzelmann (Department of Medicine, University of Fribourg, Fribourg, Switzerland), Erg6p was from Professor Günther Daum and Dr Karin Athenstaedt (Institute of Biochemistry, Graz University of Technology, Austria), and Yah1p was from Dr Doron Rapaport (Ludwig-Maximilians-Universität, Munich, Germany). The Pho8p antibody were purchased from Molecular Probes (Eugene, OR, U.S.A.) or obtained from Dr Gregory Payne (Department of Biological Chemistry, University of California, Los Angeles, CA, U.S.A.).

Purification of vacuoles and vacuole fusion assay

Cells were grown in YPD medium overnight, diluted and grown to a D_{600} of 1.0–1.2 in YPD. Vacuoles were purified by DEAE-dextran lysis and flotation in a Ficoll step-gradient, as described previously [24]. Vacuole fusion assay was performed as described in [25] using 3 μg of total protein from both vacuole preparations used in each assay. The effect of Acb1p, CoA and palmitoyl-CoA on the fusion reaction was evaluated by adding the effectors to samples before addition of vacuoles. Vacuoles devoid of lipid droplets were purified as described in [26,27].

Fluorescence microscopy

In vivo localization of GFP (green fluorescent protein) fusion proteins was evaluated by fluorescence microscopy using a Leica fluorescence microscope equipped with a PL APO 100 × 1.40 objective. Cells transformed with appropriate plasmids were grown to a D_{600} of 0.8–1.0 in selective synthetic minimal glucose medium. The plasmid carrying a C-terminal fusion of Vac8 to GFP under the control of the *CUP1* promoter was kindly provided by Dr David Goldfarb (Department of Biology, University of Rochester, NY, U.S.A.). Expression of Vac8p–GFP was induced by addition of 10 μM $CuSO_4$ 3 h before microscopy. A plasmid carrying the Nyv1–GFP fusion was kindly provided by Dr Hugh Pelham (MRC Laboratory of Molecular Biology, Cambridge, U.K.), and the Vph1–GFP plasmid was kindly given by E. Jones (Hospital for Sick Children, Toronto, Canada). The Tlg2–GFP plasmid was from Dr R. Haguenauer-Tsapis (Jacques Monod Institute, University of Paris, Paris, France). GFP was visualized using a FITC filter, whereas FM 4-64 staining was performed as described in [28] and visualized using a rhodamine filter. Images were processed using Adobe Photoshop 6.0 (Adobe, Mountain View, CA, U.S.A.).

Lipid extraction and MS analysis of lipids

Growth was stopped by addition of 0.1 vol. of ice-cold 6.6 M $HClO_4$ to the culture. Following incubation on ice for 10 min, cells were harvested by centrifugation at 3500 ***g*** for 10 min at 4 °C. The pellet was resuspended in ice-cold $HClO_4$ (10 mM), transferred to a 12 ml test tube and harvested by centrifugation. Internal standards were added directly to the pellet, if needed. The volume was adjusted to 0.4 ml with 1 M HCl, followed by addition of 1.5 ml of chloroform/methanol (1:2, v/v) and glass beads (450–600 μm). Cells were disintegrated by alternate 30 s periods of vortex-mixing and cooling on ice until cells were broken, as confirmed by microscopy. Chloroform and H_2O (0.5 ml each) were added to the homogenate, followed by vortex-mixing and phase separation by centrifugation. The lower phase was removed using a drawn Pasteur pipette, and transferred to a 4 ml silica screw-cap glass tube. Glass beads and upper phase were washed twice with 1 ml of chloroform. The chloroform washes were combined with the lower phase. The three pooled lower phases were washed with 1 M HCl (1 ml) in methanol/water (1:1, v/v) and transferred to a clean 4 ml screw-cap tube. The solvent was removed in a stream of N_2, and the dry lipids were stored at − 80 °C.

For MS experiments, lipids were dissolved in chloroform/methanol (1:2, v/v), and divided into two portions. One half was used directly for negative-mode MS. For positive-mode MS, the second half was made up to a concentration of 10 mM with ammonium acetate, pH 4.5, in order to stabilize pH.

For quantitative mass spectrometric analysis of ceramides, cells (100 D_{600} units) were harvested as described above, and bovine brain ceramides (15 nmol) were added as an internal standard to the cell pellet. Glass beads (0.5 ml) and 1 ml of ethanol/H_2O/diethyl ether/pyridine/ammonium hydroxide (25–35 %) (15:15:5:1:0.018, by vol.) were added and the cells broken by vortex-mixing as described above, the extract was transferred to a test tube and the extraction was repeated. Extracts were pooled and the solvent removed with a stream of nitrogen. The dry extract was dissolved in chloroform/methanol/H_2O (16:16:5, by vol.) (0.1 ml) and saponified with 0.2 M NaOH (1 ml) in methanol for 1 h at 30 °C, followed by the addition of 0.5 M EDTA (0.5 ml) and H_2O (0.2 ml). The unsaponified lipids were extracted with 1 ml of chloroform. The chloroform phase was removed and washed with 1 M HCl (1 ml) in methanol/water (1:1, v/v). The chloroform phase was taken to dryness under a stream of nitrogen, dissolved in chloroform/methanol (1:2, v/v) and analysed by MS, as described above.

The MS analysis was performed employing an Esquire ion trap-electrospray mass spectrometer from Bruker/Hewlett–Packard. MS data were analysed using Bruker Data analysis™ version 2.0. Nitrogen was used as the drying gas (1 litre/min at 80 °C). In the negative-ion mode, the potentials of the spray needle, capillary exit and skimmers 1 and 2 were + 600, − 134, − 52 and − 6 V,

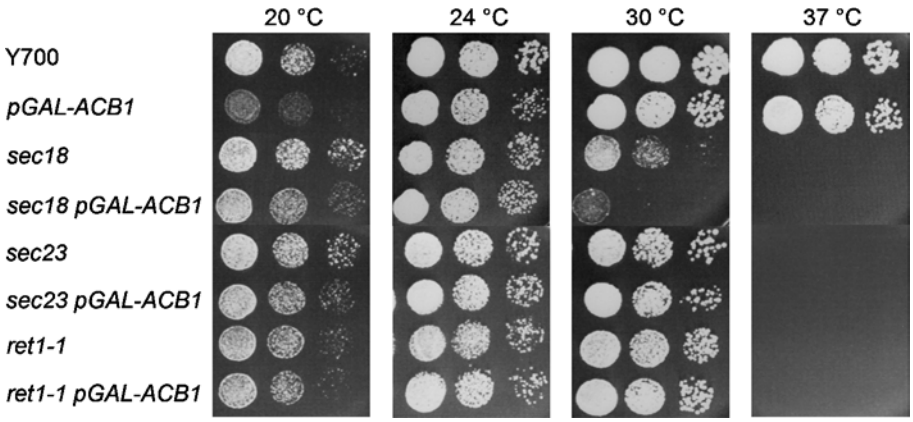

Figure 1 Depletion of Acb1p in temperature-sensitive mutants of the secretory pathway

Cells were grown in YPD overnight at 24 °C, serial-diluted in water and spotted on to YPD plates. Growth was monitored after 48 h at 20 °C, 24 °C, 30 °C and 37 °C.

respectively. In the positive-ion mode, the respective potentials were +600, +134, +52 and +6 V. Full-scan mass spectra ranging from *m/z* 50–2000 were collected in both the modes. Phosphatidylcholine and phosphatidylethanolamine species were analysed in the positive-ion mode, and the phosphatidylserine, phosphatidylinositol, ceramides and sphingolipid species in the negative ion mode. For phospholipid and ceramide/sphingolipid analysis, each ESI–MS spectrum represents an average of 50 and 300 scans respectively.

RESULTS

We have recently shown that depletion of Acb1p from *S. cerevisiae* leads to aberrant organelle and membrane structures. Acb1p-depleted cells accumulate 50–60 nm vesicles and autophagocytotic-like bodies, and show strongly perturbed plasma membrane structures [20]. To investigate how the function of Acb1p interacts with other components of the secretory machinery, we crossed the *pGAL1-ACB1* strain with strains harbouring temperature-sensitive mutations in *SEC18* [the yeast homologue of mammalian NSF (*N*-ethylmaleimide-sensitive fusion protein)], *SEC23* (COPII component, and activator of Sar1p), and *RET1* (α-COP). Sec18p is required for fusion of ER-derived vesicles to Golgi membranes, as well as for vacuolar fusion [29,30]. The *SEC23* and the *RET1* gene products are involved in the budding of COPII vesicles from the ER [31] and the formation of COPI vesicles [32] respectively. All haploid double mutants were viable, and occurred with the expected frequency after tetrad dissection. Cells were grown overnight in glucose medium, serial-diluted into fresh medium and spotted on to YPD plates, which were placed at different temperatures. At permissive temperatures (below 24 °C), all double mutants were viable. Interestingly, at 30 °C, depletion of Acb1p in the *sec18*^{ts} strain resulted in severe growth retardation (Figure 1), indicating that the non-permissive temperature for the *sec18-1* allele is lowered by depletion of Acb1p. Depletion of Acb1p in combination with inactivation of the *SEC23* and *RET1* gene products did only result in minor growth retardation (Figure 1), showing that fusion, but not budding reactions, are impaired by a reduction in Acb1p levels.

Acb1p depletion affects the morphology of the vacuole

We have previously shown that Acb1p accumulates a large number of 50–60 nm vesicles, larger vesicles, autophagocytotic-like bodies and micro-autophagocytotic vesicles inside the vacuole [20]. Expression of the vacuole proteins Vac8p and Vph1p fused to the green fluorescent protein, and analysis of their intracellular localization by fluorescence microscopy, showed that 80–90 % of the vacuoles in the mutant strain were strongly multi-lobed (Figure 2). Staining cells with the vacuolar dye FM 4-64 confirmed the multi-lobed vacuolar morphology (Figure 2). Growing cells in medium supplemented with high concentrations (500 μM) of palmitic acid, which was found to restore the decreased sphingolipid steady-state levels observed in Acb1p-depleted cells [20], restored the vacuole morphology (results not shown). To confirm that the multi-lobed appearance of the vacuoles is due to the lack of Acb1p, we restored the expression of Acb1p in the *pGAL1-ACB1* strain. The cells were transformed with an ER-V16-GAL4 plasmid, which carries a gene encoding a fusion protein between the ligand-binding domain of the oestrogen receptor and the *GAL4* DNA-binding domain [33]. This fusion protein becomes transcriptionally active upon binding of oestrogen, which enabled us to induce the expression of Acb1p under glucose-repressing conditions by adding oestrogen to the growth medium. In parallel with an increase in the expression of Acb1p, we observed that the vacuole morphology was restored to the wild-type appearance (Figure 3). The vacuole morphology was similar to wild-type vacuoles as the level of Acb1p in the mutant strain reached wild-type levels. The fact that appearance of a multi-lobed vacuole is a feature commonly shared between mutants defective in endocytotic trafficking could suggest that depletion of Acb1p also affected the delivery of FM4-64 to the vacuole compartment. Compared with wild-type cells, discrete early endosomal vesicles were not clearly visible in Acb1p-depleted cells and vacuoles were eventually stained efficiently in both strains (Figure 2, and results not shown). Furthermore, depletion of Acb1p does not affect endocytosis, as determined by binding and internalization of the α-factor–receptor complex (Howard Riezman, personal communication,). Thus, even though early endosomal vesicles were not clearly visible in Acb1p-depleted cells, endosomal trafficking from the plasma membrane to the vacuole seems not to be affected dramatically in Acb1p-depleted cells.

Acb1p depletion affects protein transport

To clarify further the extent and specificity of protein transport defects in Acb1p-depleted cells, we monitored the transport kinetics of a number of marker proteins from the *trans*-Golgi to the vacuole by pulse–chase analysis. The yeast vacuolar protein API is synthesized as a cytosolic 61 kDa precursor, which is transported

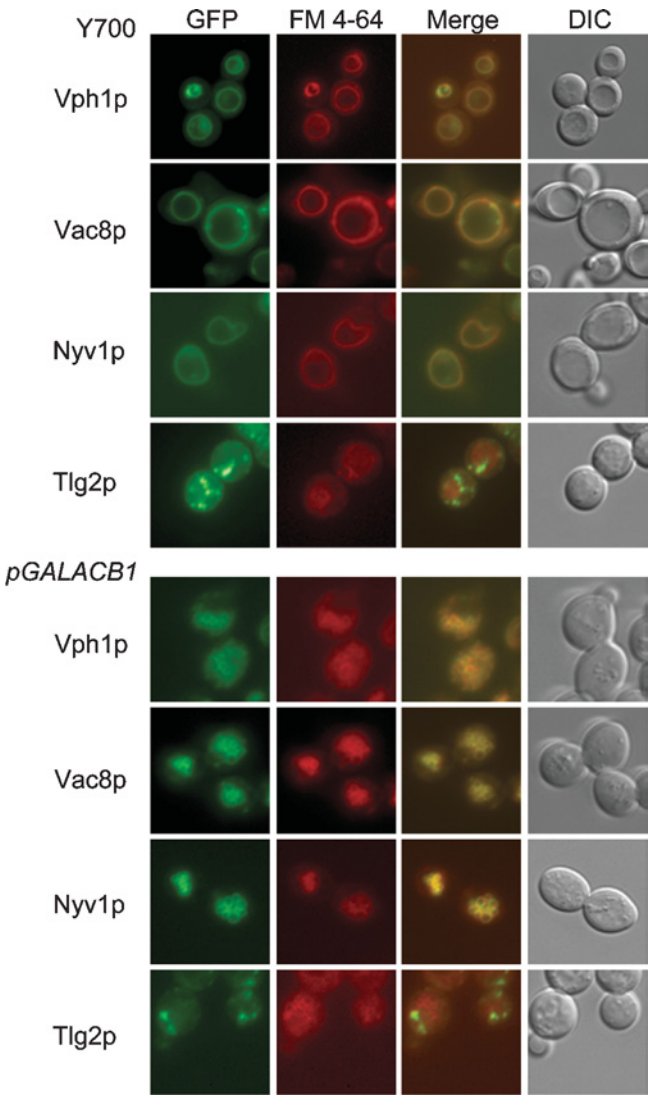

Figure 2 Multi-lobed vacuoles in cells depleted of Acb1p

The vacuole morphology was evaluated in wild-type (upper panel) and Acb1p-depleted (lower panel) cells harbouring plasmids carrying GFP fusions to Vac8p, Vph1p or Nyv1p, by staining cells with the vacuolar dye FM 4-64, and with subsequent visualization by fluorescence- and differential interference contrast-microscopy (DIC), as indicated.

to the vacuole by a non-classical vesicular-targeting mechanism called the 'cvt pathway'. In the vacuole, API is cleaved in a proteinase-B-dependent reaction, resulting in a 50 kDa mature form of API [34]. We find that the half-life of API for vacuolar delivery is increased from 35 min in wild-type cells to 80 min in cells lacking Acb1p (Figure 4A). CPY, which is transported through the vacuolar-protein-sorting pathway [35], is initially synthesized in the ER as a 67 kDa core-glycosylated proenzyme (p1), which is converted into the 69 kDa form (p2) in the Golgi by modification of the core glycosylation, and is ultimately processed to the 61 kDa mature form when it arrives in the vacuole. In cells lacking Acb1p, conversion from p1- into p2-CPY was slightly compromised, and an intermediary glycosylated p2CPY-precursor form with slower mobility was formed, giving rise to a diffuse appearance of the labelled bands. This suggests that the glycosylation of CPY in the Golgi is delayed (Figure 4A). The conversion of precursor alkaline phosphatase (pALP/Pho8p) into mature alkaline phosphatase was not affected by depletion of Acb1p (Figure 4A), and thus shows normal transport to the vacuole via the AP3 adaptor complex pathway. Transport of the GPI-anchored protein, Gas1p, from the ER to the Golgi has been shown to depend on gene products specifically required in vesicular-transport processes, and also on ceramide synthesis [36,37]. However, maturation of Gas1p was not affected by depletion of Acb1p (Figure 4A).

The appearance of a higher frequency of micro-autophagocytotic invaginations in vacuoles from Acb1p-depleted cells compared with wild-type [20] indicated that proteins might be imported to the vacuole by this route in Acb1p-depleted cells. We therefore examined whether CPY could be transported to the vacuole by micro-autophagocytosis. The t (target)-SNARE (soluble NSF attachment protein receptor) Vam3p is obligatory for transport to the vacuole through the vacuolar-protein-sorting pathway and the cvt pathway [38], but is not required in micro-autophagocytosis [39]. To answer this question, we repeated the pulse–chase analysis in a Vam3^{tsf} (Vam3 temperature-sensitive) background at both the permissive and non-permissive temperature. CPY maturation in Y700*vam3*^{tsf} and Y700 *pGAL1-ACB1 vam3*^{tsf} is very similar at the permissive temperature. However, when grown at non-permissive temperature, maturation of CPY was slightly more delayed in the Acb1p-depleted strain (Figure 4A), confirming that CPY transport is slightly compromised in this strain. We repeatedly found that API maturation is compromised in Acb1p-depleted cells in the wild-type genetic background at 30 °C. However, maturation of API at permissive temperature

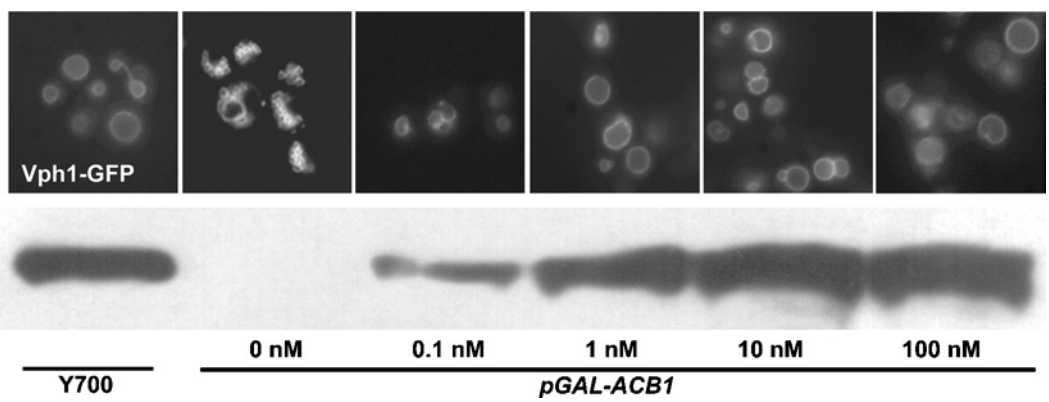

Figure 3 The multi-lobed vacuoles are due to the lack of Acb1p

The morphology of the vacuole was evaluated in cells co-transformed with plasmids carrying genes encoding the Vph1–GFP fusion protein and an ER-GAL4 fusion protein, respectively. Upon activation of the ER-GAL4 fusion protein by the addition of oestrogen, expression of Acb1p increases, as shown by Western blotting and the vacuolar morphology becomes normalized.

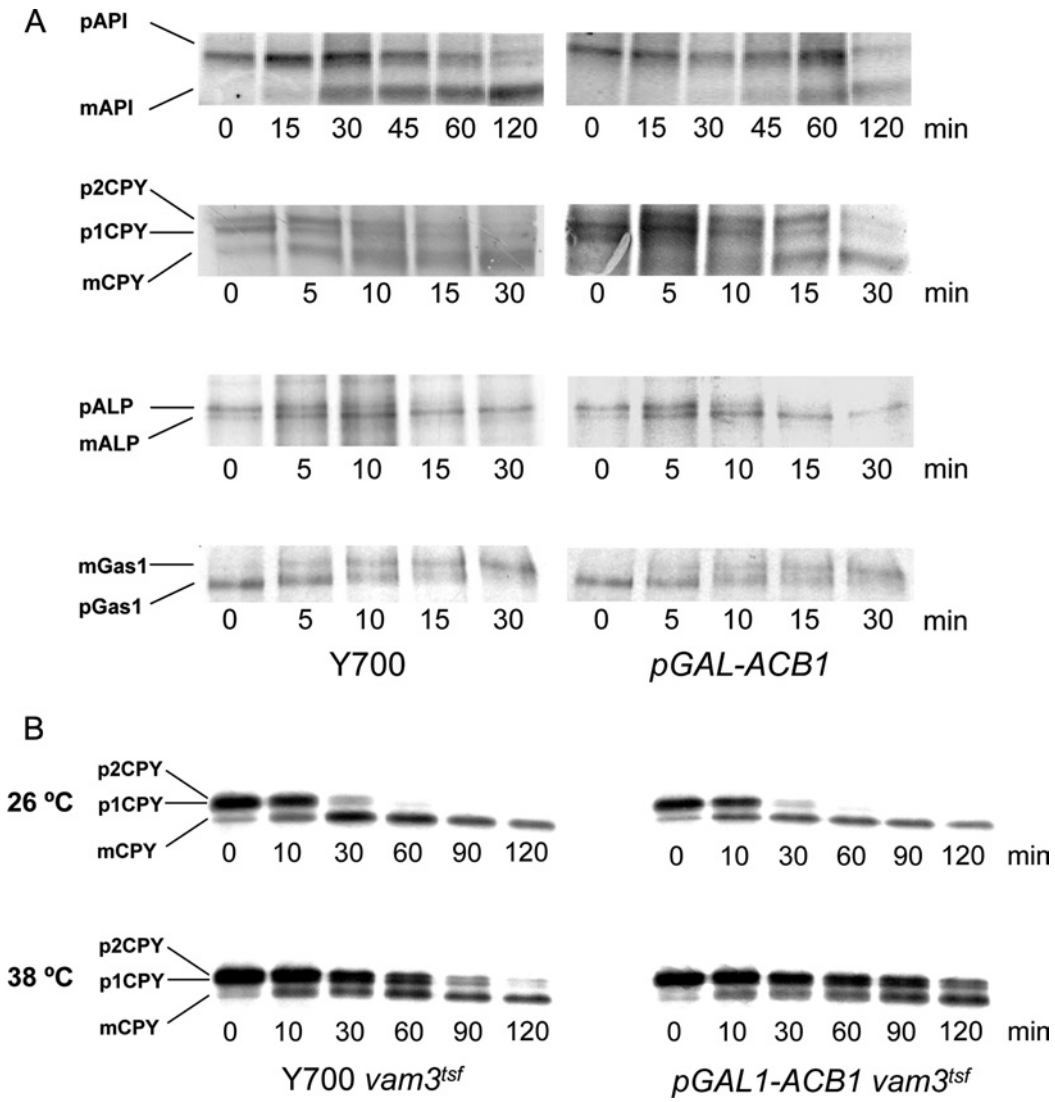

Figure 4 Protein maturation is affected by the absence of Acb1p

(**A**) Pulse–chase analysis of wild-type (Y700) or *pGAL-ACB1* cells show that API maturation is compromised, whereas maturation of CPY is slightly affected. Maturation of ALP and Gas1p is unaffected. (**B**) Pulse–chase analysis of Vam3^{tsf} and *pGAL-ACB1* Vam3^{tsf} cells shows that inactivation of Vam3p affects CPY maturation in Acb1p-depleted cells.

(26 °C) in Y700*vam3^{tsf}* and Y700 *pGAL1-ACB1 vam3^{tsf}* did not differ (results not shown). This may be due to the fact that overall transport to the vacuole is reduced both in a Vam3^{tsf} background and at 26 °C. At the non-permissive temperature (38 °C), the maturation of API was completely blocked in the Vam3^{tsf} background. This shows that, despite Acb1p depletion, API transport to the vacuole is completely dependent on Vam3p. Thus this makes it unlikely that micro-autophagocytosis plays a significant role in protein transport to the vacuole in Acb1p-depleted cells.

In conclusion, the loss of Acb1p affects API and CPY transport to the vacuole in a wild-type background, but not in a Vam3p^{tsf} background at the permissive temperature. At the non-permissive temperature, API maturation is completely blocked in both strains, whereas CPY maturation is slightly compromised. ALP maturation was not affected by depletion of Acb1p.

Homotypic vacuole fusion is defective upon depletion of ACBP

Homotypic vacuole fusion renders *S. cerevisiae* capable of maintaining vacuoles as low-copy-number organelles. On the basis of genetic and cytological studies, it is known that, upon cell division, the mother cell vacuole forms a membranous tubulovesicular structure, which elongates into the bud and delivers vacuolar material to establish the vacuole of the daughter cell. The last discernible step of vacuole inheritance is the fusion of vacuoles in the daughter cells, giving rise to one or a few vacuoles per cell. Haas and Wickner [7] reported that homotypic vacuole fusion was stimulated by the addition of myristoyl- and palmitoyl-CoA, but not by short-chain CoA esters and very-long-chain acyl-CoA esters. We therefore examined whether Acb1p is required for homotypic vacuole fusion. Homotypic vacuole fusion is routinely monitored by mixing vacuoles isolated from two different strains, one carrying a deletion in the *PEP4* gene, encoding the vacuolar luminal PrA (proteinase A), and the other carrying a deletion of the gene encoding the vacuolar membrane ALP/Pho8p [24]. Neither vacuole population harbours ALP activity, since Pho8p is imported into the vacuole as an inactive precursor, proPho8p. Provided that fusion occurs, proPho8p from the *pep4* strain is activated by PrA from the *pho8* strain.

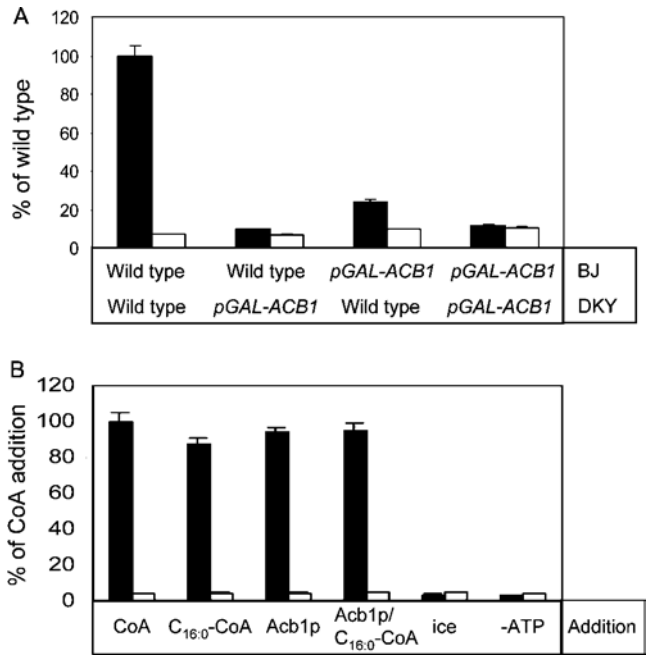

Figure 5 Homotypic vacuole fusion in Acb1p-depleted cells

(**A**) Vacuoles were isolated from strains indicated in the lower panel, and fusion was examined by mixing *pep4Δ* and *pho8Δ* vacuoles from the BJ2168 and DKY6281 cells, respectively (3 μg of each preparation) as described in the Materials and methods section. Filled-in and open bars indicate the fusion activity in standard fusion reactions allowed to proceed at 26 °C or on ice respectively. Fusion activity is expressed as the percentage of the fusion activity observed with wild-type vacuoles, which corresponds to an A_{400} of 0.33. Depletion of Acb1p renders the vacuoles incapable of undergoing homotypic vacuole fusion *in vitro*. The data shown are means $\pm$ S.E.M. for three independent experiments. (**B**) Palmitoyl-CoA alone (10 μM) or Acb1p (12 μM) in the absence or presence of palmitoyl-CoA (10 μM) was added to the vacuole fusion assay containing vacuoles isolated from the BJ2168- and DKY6281 wild-type strains (filled-in bars) or isolated from the BJ2168 strain (wt) and DKY6281-pGAL-ACB1 strain (open bars). Fusion activity is expressed as the percentage of the fusion activity observed with wild-type vacuoles incubated with 10 μM CoA, which corresponds to an A_{400} of 0.26. The data shown are the means $\pm$ S.E.M. for three independent experiments. The impaired fusion between wild-type vacuoles and Acb1p-depleted vacuoles cannot be restored by the addition of Acb1p, $C_{16:0}$-CoA or the Acb1p–$C_{16:0}$-CoA complex.

We conditionally knocked out the *ACB1* gene by inserting the *GAL1* promoter in front of the *ACB1* gene in the strains (BJ2168 and DKY6281) commonly used to measure homotypic vacuole fusion. Depletion of Acb1p did not affect the level of either Pho8p or Pep4p in isolated vacuoles (see below). Vacuoles, derived from either glucose-grown BJ2168 *pGAL-ACB1* or DKY6281 *pGAL-ACB1*, were unable to fuse with the corresponding wild-type vacuoles in standard fusion reactions. The resulting fusion activity was close to wild-type vacuole fusion activity in the absence of ATP or in control incubation on ice (Figure 5A). Low fusion levels were also observed when Acb1p had been depleted from both strains prior to isolation of vacuoles. Similar results were obtained when *PEP4* or *PHO8* was deleted in the Y700 or Y700 *pGAL-ACB1* strains, respectively (N. Færgeman, J. Knudsen and C. Ungermann, unpublished work). One interpretation of these results is that the Acb1p–acyl-CoA complex is essential for donating the acyl-CoA esters required for homotypic vacuole fusion. However, addition of CoA, palmitoyl-CoA, Acb1p or the Acb1p–palmitoyl-CoA complex (in a ratio of 1:2) failed to restore fusion between wild-type vacuoles and vacuoles isolated from the Acb1p-depleted strain (Figure 5B). These observations therefore indicate that Acb1p and/or the acyl-CoA is not involved in the actual fusion event itself, but rather in the assembly of the vacuole fusion machinery in the correct manner.

Assembly of vacuoles requires Acb1p

We examined whether the vacuolar morphology and the relative levels of vacuole marker proteins Vac8p, API, PrA and Pho8p (ALP), and the levels of the two v (vesicular)-SNAREs Nyv1p and Vti1p and the t-SNARE Vam3p, are altered in vacuoles isolated from Acb1p-depleted cells compared with wild-type vacuoles. Using the standard Ficoll step-gradient and ultracentrifugation, vacuoles were isolated from wild-type cells and from cells depleted of Acb1p. Staining of isolated vacuoles with FM 4-64 clearly showed that vacuoles from Acb1p-depleted cells were enlarged in size and clustered compared with wild-type vacuoles (Figure 6A). The level of the selected vacuolar proteins was determined by immunoblotting. Steady-state levels of the vacuole marker proteins Vac8p, API, PrA and Pho8p (ALP) were unaffected by the absence of Acb1p (Figure 6B). In contrast, the level of the two v-SNAREs Nyv1p and Vti1p was significantly lower in vacuoles isolated from an Acb1p-depleted strain, and the t-SNARE Vam3p was almost absent from Acb1p-depleted vacuoles (Figure 6B). In contrast, the levels of these SNARE proteins were similar in whole-cell extracts (Figure 6B), suggesting that the SNARE proteins are not properly attached to the vacuole membrane.

To examine the intracellular localization of vacuolar proteins further, we labelled cells expressing various GFP fusion proteins with FM 4-64. Vph1-, Vac8- and Nyv1 GFP fusion proteins were all found to be associated with the vacuole membrane in wild-type cells, and with both intact and multi-lobed vacuoles in Acb1p-depleted cells (Figure 2). Since all the GFP fusion proteins examined, except for the Tlg2–GFP, co-localized to the same vacuolar structures, which were stained by FM 4-64 in both wild-type and *pGAL-ACB1* cells, we believe that some of the multi-lobed vacuolar structures that are formed in the absence of Acb1p disintegrate upon isolation of the vacuoles, so that a very heterogeneous population of vacuoles are isolated from Acb1p-depleted cells. Thus this supports the suggestion that Acb1p is not required for protein sorting to the vacuole, but is required for proper attachment of components of the fusion machinery in the correct configuration to complete homotypic vacuole fusion.

Acb1p-depleted cells have a lower ceramide content

In an effort to examine whether the differences in vacuole fusion are caused by changes in the lipid composition, we analysed the lipid composition in vacuoles isolated from either wild-type cells or Acb1p-depleted cells by ESI–MS. The isolated vacuoles were highly enriched for Vac8p, and contained only trace amounts of lipid bodies (Erg6p) and mitochondrial matrix (Yah1p; Figure 7A). The plasma-membrane marker Gas1p was present in vacuoles isolated from both wild-type and Acb1p-depleted cells, but was not enriched in them, as was Vac8p. The Golgi- and the ER-markers, Kex2p and Sec12p respectively, could not be detected in the isolated vacuoles. ESI–MS analysis revealed an increase in the level of glycerophospholipids containing shorter and more unsaturated acyl-chains (C16:0; C16:1 or C16:1; C16:1) in Acb1p-depleted cells (Figure 7B). Acyl-CoA esters are precursors for synthesis of both VLCFAs (very-long-chain fatty acids) and PHS (phytosphingosine), which are both required for sphingolipid biosynthesis (Figure 8). Four independent experiments showed that the ceramide PHS-C18-26-OH (ceramide C; see Figure 8) is completely undetectable in vacuoles isolated from Acb1p-depleted cells by ESI–MS analysis

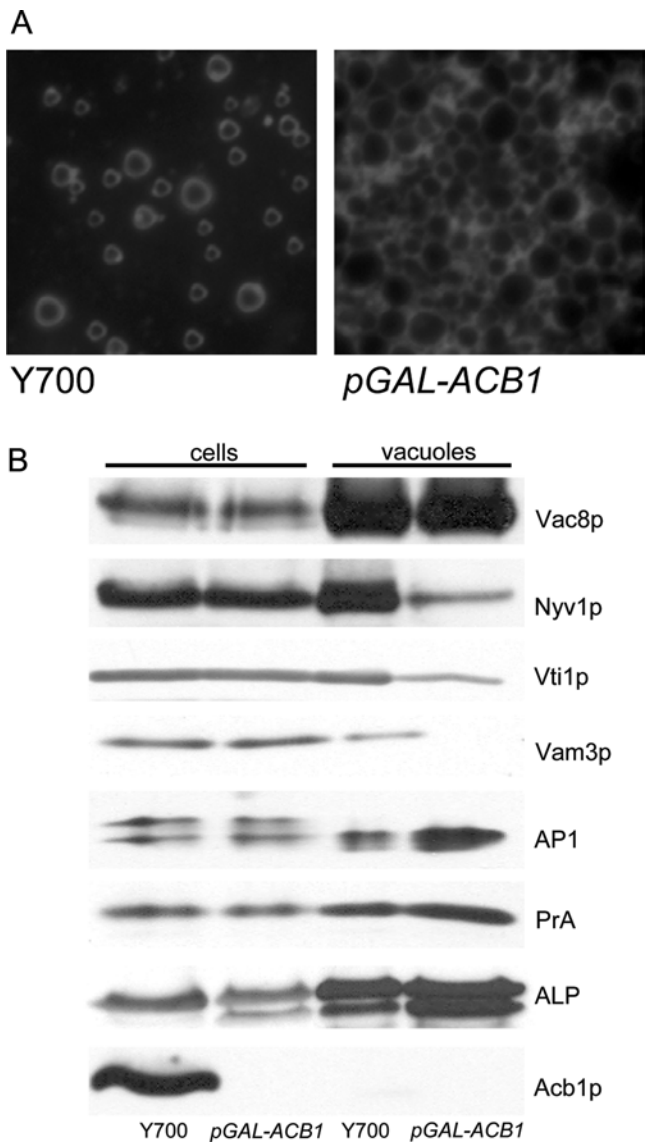

Figure 6 Depletion of Acb1p from cells affects the morphology of isolated vacuoles and results in mislocalization of a number of vacuolar marker proteins

(**A**) Vacuoles, similar to the vacuoles used in the fusion assay, were stained with FM 4-64 and visualized by fluorescence microscopy. Vacuoles isolated from wild-type cells are clearly homogeneous in size, whereas the vacuoles isolated from Acb1p-depleted cells are heterogeneous and enlarged in size. (**B**) The presence of vacuole proteins was examined either in total-cell extracts (corresponding to 0.1 D_{600} unit) or in isolated vacuoles (1 μg) by Western blotting using antibodies against specific vacuole proteins, as described in the Materials and methods section. The content of Nyv1p, Vam3p, and Vti1p in vacuoles isolated from Acb1p-depleted cells is considerably reduced compared with the level in vacuoles isolated from wild-type cells (Y700). Vam3p can be seen in isolated vacuoles from Acb1p-depleted cells after a longer period of exposure (results not shown).

(Figure 7C). The complete absence of ceramide in the vacuoles isolated from Acb1p-depleted cells cannot solely be explained by the difference in plasma membrane contamination, since the ratio between the levels of Gas1p in the two vacuole preparations is 1:4, as determined by Western blotting and densitometry scanning. Further analysis showed that the relative level of the PHS-C18-26-OH ceramide peak is 2–4 times lower in total lipid extracts from Acb1p-depleted cells compared with that in wild-type cell extracts (Figure 7C). Quantitative analysis of ceramide content in wild-type and Acb1p-depleted cells using bovine brain ceramides as an internal standard shows that both PHS-C18-C26:0-OH (ceramide-C) and PHS-C20-C26:0-OH ceramide content is 3–5-fold lower in Acb1p-depleted cells (Figure 7D). A detailed analysis of the obtained spectra showed that there is no corresponding increase in ceramide species with shorter fatty-acyl chains.

All ceramide synthesis mutant strains show fragmented vacuoles

The observation that the ceramide level is significantly reduced in whole-cell extracts, and that ceramide is undetectable in vacuoles isolated from Acb1p-depleted cells, indicates that this could be the major cause of the observed defects in vacuole structure and fusion. To investigate this further, the vacuole structure and ceramide levels in other ceramide synthesis mutants were examined. Strains carrying a temperature-sensitive allele of the palmitoyl-CoA/serine transferase Lcb1p required for synthesis of the ceramide precursor DHS (dehydrosphingosine) have been reported to have lowered ceramide content, even at the permissive temperature [40]. When compared with the W303a and Y700 wild-type strains, the ceramide level is 4 times lower in the *lcb1*^{tsf} strain and is undetectable in a *lag1*Δ*lac1*Δ strain (results not shown). FM 4-64 staining showed that vacuoles in *lcb1*^{tsf} cells are multi-lobed at the permissive temperature (24 °C). The *lag1*Δ*lac1*Δ strain showed very diffuse staining, with the absence of clear definable vacuoles (Figure 9).

DISCUSSION

We have previously shown that depletion of Acb1p in *S. cerevisiae* results in severe perturbations in membrane morphology and assembly, including accumulation of vesicles, membrane fragments and multi-layered plasma membrane structures [20]. This prompted us to analyse further the role of acyl-CoA-binding protein, Acb1p, in vesicular trafficking and vacuole fusion. Pfanner et al. [9] showed that acyl-CoA esters are needed in the attachment and uncoating of transport vesicles. Long-chain acyl-CoA esters have also been shown to be required for homotypic vacuole fusion in *S. cerevisiae* [7]. Consistent with the observation by Pfanner et al. [9], the stimulatory effect was dependent on the presence of a functional NSF/Sec18p. Interestingly, Sec18p mediated priming was also required for palmitoylation of Vac8p [23]. However, the present observation that depletion of Acb1p does not significantly affect growth of *sec23* and *ret1-1* mutants at the restrictive temperature (Figure 1) implies that Acb1p is not ubiquitously required in the protein-trafficking process, but rather in distinct steps within or processes required by the secretory pathway. This is supported by the pulse–chase analysis, showing that only maturation of API, and to a lesser degree also of CPY, and not maturation of Gas1p and ALP are affected by depletion of Acb1p (Figure 4). It is therefore interesting that depletion of Acb1p in a *sec18* temperature-sensitive strain abolished growth at 30 °C (Figure 1), strongly implying that Acb1p is required for Sec18p-dependent vesicular fusion. The inability of vacuoles isolated from Acb1p-depleted cells to undergo homotypic vacuole fusion *in vitro* (Figure 5) is consistent with the notion that Acb1p is involved in membrane assembly and trafficking, as indicated previously [20]. However, the inability of acyl-CoA alone or in complex with Acb1p to complement the defect in homotypic vacuole fusion *in vitro* indicates that Acb1p may not only be required in the fusion process itself, but also in an upstream process required for vacuole fusion. Vacuoles isolated by flotation from Acb1p-depleted cells are clearly very heterogeneous in size (Figure 6A). These vacuoles contain strongly reduced amounts of the SNAREs Vam3p, Vti1p and Nyv1p than wild-type vacuoles,

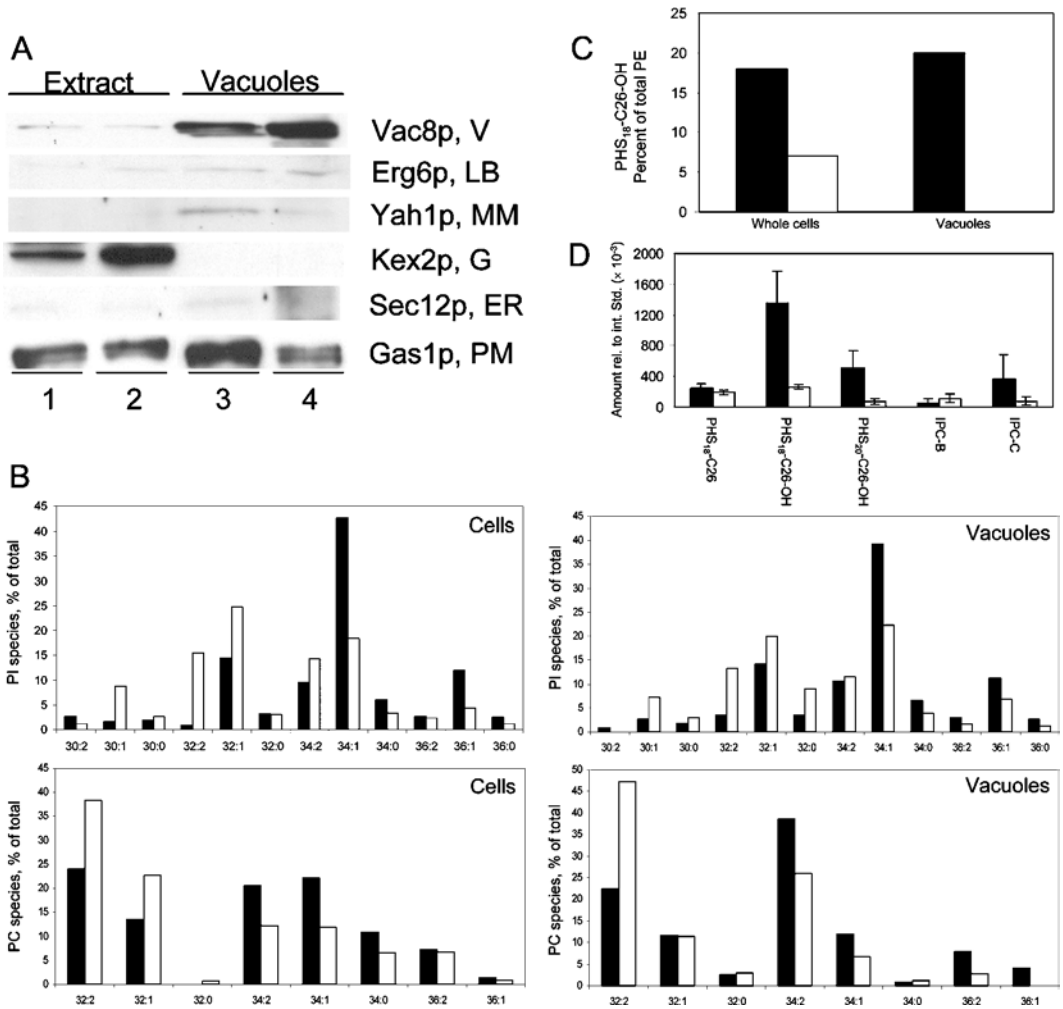

Figure 7 Marker analysis of the isolated vacuoles (A), ESI–MS analysis of whole-cell or vacuolar glycerophosphatidylinositol or glycerophosphatidylcholine species from wild-type or Acb1p-depleted cells (B), ESI–MS analysis of unsaponified lipids extracted from total cellular lipids or vacuolar lipids from wild-type or Acb1p-deplated cells (C) and ESI–MS analysis of ceramides in Acb1p-depleted cells (D)

Vacuoles were isolated as described in the Materials and methods section. The presence of organelle-specific marker proteins in total-cell extracts (1 μg, except for Kex2p analysis, where 10 μg was used) or isolated vacuoles (1 μg) from wild-type (lanes 1 and 3) or Acb1p-depleted (lanes 2 and 4) cells were examined by Western blotting using the indicated antibodies. V, vacuoles; LB, lipid bodies; MM, mitochondrial matrix; G, Golgi; ER, endoplasmic reticulum; PM, plasma membranes. (**B**) Whole-cell or vacuolar glycerophosphatidylinositol or glycerophosphatidylcholine species from either wild-type (filled-in bars) or Acb1p-depleted (open bars) cells were analysed by ESI–MS as described in the Materials and methods section. The amount of each species has been calculated relative to the total amount of each individual phospholipid class. The mean for two independent experiments is shown. (**C**) Unsaponified lipids extracted from total cellular lipids or vacuolar lipids from either wild-type (filled-in bars) or from Acb1p-depleted cells (open bars) were analysed by ESI–MS, as described in the Materials and methods section. The relative amount of PHS_{18}-C26-OH in each fraction analysed has been calculated relative to the total amount of phosphatidylethanolamine in each fraction. The data shown are representative of four independent experiments. (**D**) Quantitative analysis of ceramides in Acb1p-depleted cells by ESI–MS. After mild base saponification, unsaponified lipids from wild-type (filled-in bars) or Acb1p-depleted (open bars) cells were analysed by ESI–MS, as described in the Materials and methods section. The amount of each species has been calculated relative to the amount of internal standard added. The data shown are means $\pm$ half the difference for two independent experiments.

despite the fact that the levels in total-cell extracts are similar (Figure 6B). This supports the notion that Acb1p is required in a step upstream even of the actual fusion. This, and the observation that Vph1–, Vac8– and Nyv1–GFP were found to co-localize with FM 4-64 in both normal and multi-lobed vacuoles in Acb1p-depleted cells, indicate that these proteins are delivered to vacuoles in Acb1p-depleted cells. This is consistent with the notion that ALP maturation is unaffected by depletion of Acb1p (Figure 4A), and that both ALP and Vam3p are transported to the vacuole via the AP3 pathway [41]. Compared with total wild-type cell extracts, similar amounts of Vam7p and Vti1p co-immunoprecipitate with Nyv1p in cells depleted of Acb1p, indicating that assembly and disassembly of SNARE complexes occurs in a normal fashion (results not shown). However, the fact that the SNARE proteins are lost from vacuoles isolated from the Acb1p-depleted cells suggests that the complexes are not correctly attached or integrated into the vacuole membrane. Despite the altered vacuole morphology and block in vacuole fusion, Acb1p-depleted cells segregate vacuoles into daughter cells properly (results not shown), phenotypic features which are also seen upon inactivation of Vam3p [38,42]. All together, these data indicate that delivery of fusion components to the vacuole occurs in the correct manner, despite the lack of Acb1p, but that the correct assembly of a functional fusion machinery is compromised, resulting in a block in vacuole fusion and multi-lobed vacuoles.

Depletion of Acb1p does not affect endocytosis, as determined by binding and internalization of the α-factor–receptor complex.

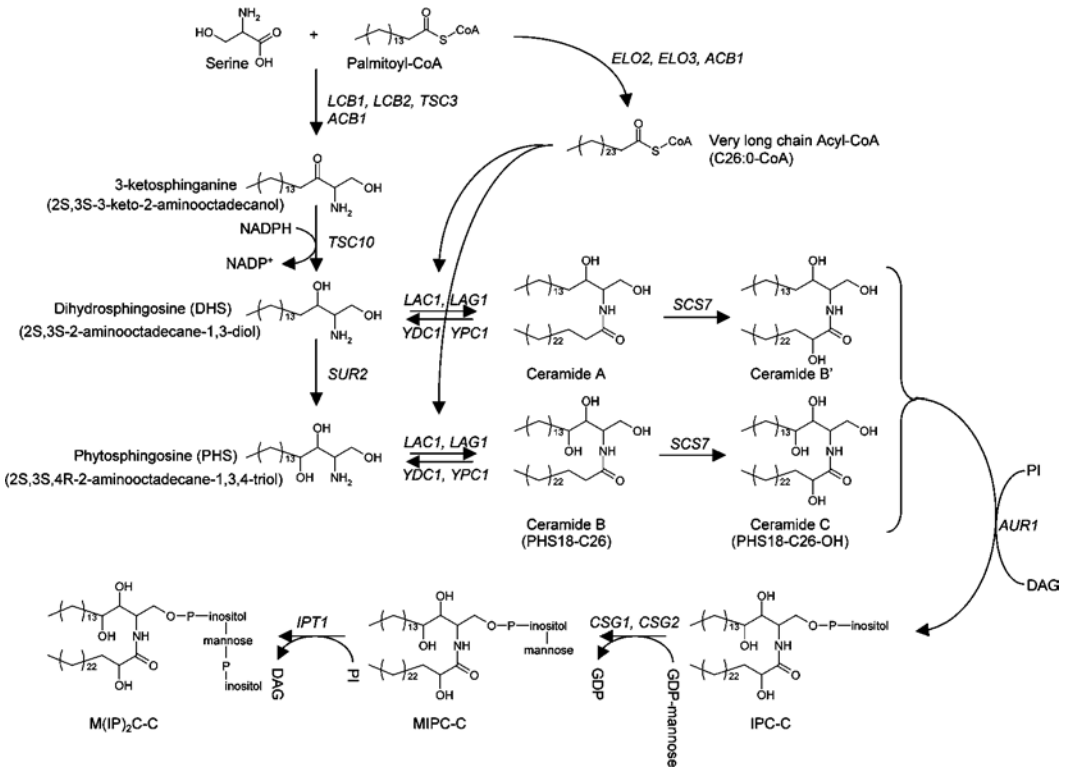

Figure 8 Biosynthesis of ceramides and sphingolipids in *S. cerevisiae*

Gene names are shown in italics. The metabolism of phosphorylated long-chain bases (P-DHS and P-PHS) is not shown. The systematic name of each long-chain base is shown below its common name. The shown PHS is PHS18. Only the synthesis of IPC-C is shown. The synthesis of IPC-A, IPC-B and IPC-D occurs in a similar manner from the respective ceramides.

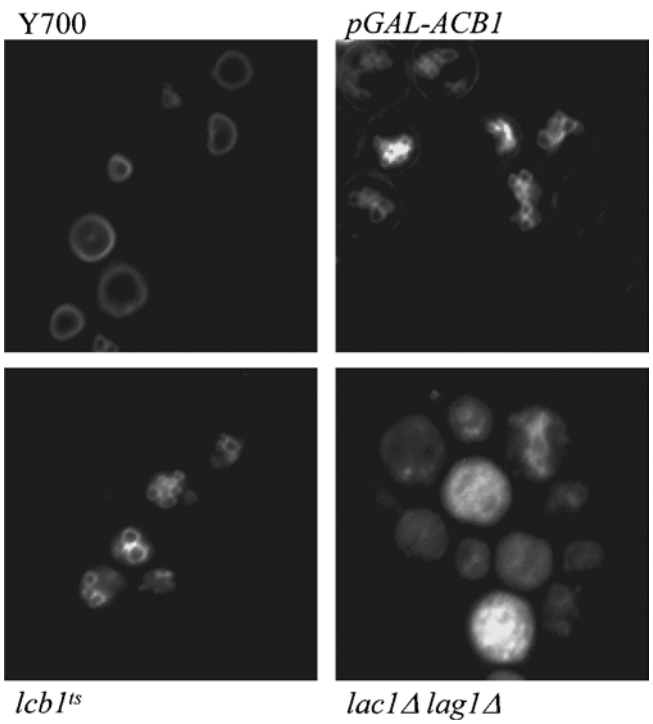

Figure 9 Vacuolar morphology in ceramide synthesis mutants

Cells were grown in YPD medium to exponential phase at 30 °C, except for the *lcb1*^{ts} strain, which was kept at 24 °C at all times. Cells were then labelled with FM 4-64, as described in the Materials and methods section, and analysed by fluorescence microscopy.

This, and the fact that transport of FM 4-64 to the vacuole appears not to be dramatically affected in Acb1p-depleted cells, suggests that trafficking to the vacuole is only moderately affected by Acb1p depletion. The most pronounced effect of Acb1p depletion is a gross alteration in overall membrane and organelle structure, implying that the effect may be caused by major alterations in the membrane lipid compositions.

We have previously shown that the plasma membrane levels of lysophosphatidic acid, lysophosphatidylserine and lysophosphatidylinositol are, respectively, 1.71-, 1.93- and 2.16-fold higher in plasma membranes isolated from cells depleted of Acb1p [20]. That study also showed that the synthesis of IPC (inositolphosphoceramide) is strongly compromised in Acb1p-depleted cells, although the levels of IPC and mannosyl-IPC were 40 % increased in the plasma membrane relative to phosphatidylinositol. Could Acb1p be involved in membrane remodelling or synthesis of specific lipids required for membrane function and fusion? The fact that loss of phosphatidylserine synthesis leads to aberrant vacuolar morphology [43], and that ergosterol is required for homotypic vacuole fusion [44], underline the importance of specific lipids in controlling organelle assembly, function and morphology.

The ESI–MS analysis clearly demonstrates that ceramide is absent from vacuoles isolated from Acb1p-depleted cells. Using bovine brain ceramides as an internal standard, it was shown that Acb1p-depleted cells have strongly reduced levels of ceramide and IPC-C compared with wild-type cells. It is also interesting that wild-type cells contain mainly IPC-C, in contrast with the Acb1p-depleted cells, which contain equal amounts of IPC-C and IPC-B, indicating that α-hydroxylation of ceramide is also compromised in Acb1p-depleted cells.

Other ceramide synthesis mutants with lowered ceramide levels also show vacuole morphology defects similar to those of Acb1p-depleted cells (Figure 9). Interestingly, vacuoles could not be visualized by FM 4-64 staining in the *lag1Δlac1Δ* strain, which is devoid of normal ceramide synthesis [45,46], indicating that ceramides are required for formation of normal vacuoles. We therefore suggest that reduced ceramide levels may be the primary cause for the defect in the overall membrane organization, including vacuole structure and vacuole fusion in Acb1p-depleted cells. It has recently been shown that the vacuole membrane ATPase requires the presence of sphingolipids in the vacuole [47]. However, depletion of Acb1p does not affect vacuole acidification (results not shown). Ceramide and sphingolipid synthesis is required for raft formation and plasma membrane association of Pma1p and Fur4p [48,49]. We therefore suggest that ceramides/sphingolipids, in a similar way, are required for the formation of specific lipid domains on the vacuole required for proper integration and function of the fusion complex.

It is interesting to note that Gas1p transport and maturation, which has been reported to depend on ongoing ceramide synthesis [5], is unaffected by Acb1p depletion, despite the lowered ceramide levels in these cells (Figure 4A). This indicates that ceramide synthesis at the ER level is sufficient to support Gas1p transport, suggesting that ceramide synthesis occurs independently at different locations at the same time, and that these sites are differently affected by Acb1p depletion. Ceramide synthesis specifically requires C26 fatty acids, and is therefore dependent on the fatty acid elongation pathway. It is therefore interesting that Tsc13p, Elo2p and Elo3p, all components of the fatty acid elongation complex, localize to the ER, but are also enriched at nuclear–vacuole junctions [50]. Furthermore, it was shown that Tsc13p–GFP-containing vesicles are found to be closely associated, or even enclosed, by FM4-64 stained vacuole structures. The very low solubility of VLCFA-CoAs is likely to imply a concerted metabolic channelling mechanism from the site of synthesis to their subsequent incorporation into ceramides by ceramide synthetase. We therefore suggest that Acb1p is required for donation of palmitoyl-CoA for the synthesis of ceramide precursors (either VLCFA-CoA and/or long-chain bases) at specific locations. This could include distinct ceramide synthesis at the nuclear–vacuole junction, which also explains the absence of ceramide from vacuoles isolated from Acb1p-depleted cells.

In conclusion, the present results strongly imply that Acb1p is required for normal ceramide synthesis, and that the presence of ceramides in the vacuole is required for the formation of specific membrane domains, which serve to integrate the SNARE complex in the vacuole membrane and proper vacuole fusion. Although the primary cause of the defective vacuole structure and fusion can be assigned to reduced ceramide synthesis, it does not exclude that Acb1p might be required for the fusion process itself. The fact that long-chain acyl-CoA esters have been shown to be required for vacuole fusion *in vitro* is suggestive of the fact that this could be the case. The likely cause for the reduced ceramide levels in the Acb1p-depleted strain is not known at present. We suggest that Acb1p might be required for delivery/donation of *de novo*-synthesized palmitoyl-CoA to the initial step in long-chain-base synthesis catalysed by palmitoyl-CoA serine transferase (Lcb1p) and/or the fatty acid elongation system (Elo2p and Elo3p). The observation that Acb1p-depleted cells contain 30–40% less C26 fatty acid [20] supports the suggestion that reduced fatty acid elongation could be a contributing factor to lowered ceramide synthesis. We are currently investigating these possibilities. Finally, it should also be considered that altered protein acylation could be an additional contributing factor causing membrane morphology defects in Acb1p-depleted cells.

The observation that human, mouse and insect ACBPs can complement growth defects and vacuole morphology in Acb1p-depleted cells (results not shown) suggests that Acb1p/ACBP supports similar functions in all eukaryotes, and that yeast is a valid model system for studying the function of ACBPs from higher eukaryotes.

This work was supported by The Deutsche Forschungsgemeinschaft, The Danish Natural Science Council and Møllerens Fond. We gratefully acknowledge the receipt of antibodies and/or yeast strains from Professor Lois Weisman, Professor Susan Ferro-Novick, Professor Daniel Klionsky, Dr Jakob Winther, Professor Scott Emr (Department of Cellular and Molecular Medicine, Howard Hughes Medical Institute, UCSD School of Medicine, CA, U.S.A.), Dr Gregory Payne and Professor Andreas Conzelmann, and GFP plasmids from Dr David Goldfarb, Dr Hugh Pelham, E. Jones and Dr R. Haguenauer-Tsapis. We also wish to thank Hans Kristian Bach and Helena Christensen for excellent technical assistance.

REFERENCES

1 Cook, N. R. and Davidson, H. W. (2001) *In vitro* assays of vesicular transport. Traffic **2**, 19–25
2 Roth, M. G. (1999) Lipid regulators of membrane traffic through the Golgi complex. Trends Cell Biol. **9**, 174–179
3 Mayer, A. (2002) Membrane fusion in eukaryotic cells. Annu. Rev. Cell Dev. Biol. **18**, 289–314
4 Obeid, L. M., Okamoto, Y. and Mao, C. (2002) Yeast sphingolipids: metabolism and biology. Biochim. Biophys. Acta **1585**, 163–171
5 Sutterlin, C., Doering, T. L., Schimmoller, F., Schroder, S. and Riezman, H. (1997) Specific requirements for the ER to Golgi transport of GPI-anchored proteins in yeast. J. Cell Sci. **110**, 2703–2714
6 Færgeman, N. J., Ballegaard, T., Knudsen, J., Black, P. N. and DiRusso, C. (2000) Possible roles of long-chain fatty acyl-CoA esters in the fusion of biomembranes. Subcell. Biochem. **34**, 175–231
7 Haas, A. and Wickner, W. (1996) Homotypic vacuole fusion requires Sec17p (yeast α-SNAP) and Sec18p (yeast NSF). EMBO J. **15**, 3296–3305
8 Pfanner, N., Orci, L., Glick, B. S., Amherdt, M., Arden, S. R., Malhotra, V. and Rothman, J. E. (1989) Fatty acyl-coenzyme A is required for budding of transport vesicles from Golgi cisternae. Cell **59**, 95–102
9 Pfanner, N., Glick, B. S., Arden, S. R. and Rothman, J. E. (1990) Fatty acylation promotes fusion of transport vesicles with Golgi cisternae. J. Cell Biol. **110**, 955–961
10 Ostermann, J., Orci, L., Tani, K., Amherdt, M., Ravazzola, M., Elazar, Z. and Rothman, J. E. (1993) Stepwise assembly of functionally active transport vesicles. Cell **75**, 1015–1025
11 Pan, X. and Goldfarb, D. S. (1998) YEB3/VAC8 encodes a myristylated armadillo protein of the *Saccharomyces cerevisiae* vacuolar membrane that functions in vacuole fusion and inheritance. J. Cell Sci. **111**, 2137–2147
12 Wang, Y. X., Catlett, N. L. and Weisman, L. S. (1998) Vac8p, a vacuolar protein with armadillo repeats, functions in both vacuole inheritance and protein targeting from the cytoplasm to vacuole. J. Cell Biol. **140**, 1063–1074
13 Weigert, R., Silletta, M. G., Spano, S., Turacchio, G., Cericola, C., Colanzi, A., Senatore, S., Mancini, R., Polishchuk, E. V., Salmona, M. et al. (1999) CtBP/BARS induces fission of Golgi membranes by acylating lysophosphatidic acid. Nature (London) **402**, 429–433
14 Schmidt, A., Wolde, M., Thiele, C., Fest, W., Kratzin, H., Podtelejnikov, A. V., Witke, W., Huttner, W. B. and Soling, H. D. (1999) Endophilin I mediates synaptic vesicle formation by transfer of arachidonate to lysophosphatidic acid. Nature (London) **401**, 133–141
15 Mandrup, S., Færgeman, N. J. and Knudsen, J. (2003) Structure, function and phylogeny of acyl-CoA binding protein. In Cellular Proteins and their Fatty Acids in Health and Disease, (Duttaroy, A. K. and Spener, F., eds.), pp. 151–172, Wiley-VCH Verlag, Weinheim, Germany
16 Kragelund, B. B., Knudsen, J. and Poulsen, F. M. (1999) Acyl-coenzyme A binding protein (ACBP). Biochim. Biophys. Acta **1441**, 150–161
17 Færgeman, N. J. and Knudsen, J. (1997) Role of long-chain fatty acyl-CoA esters in the regulation of metabolism and in cell signalling. Biochem. J. **323**, 1–12
18 Rasmussen, J. T., Færgeman, N. J., Kristiansen, K. and Knudsen, J. (1994) Acyl-CoA-binding protein (ACBP) can mediate intermembrane acyl-CoA transport and donate acyl-CoA for β-oxidation and glycerolipid synthesis. Biochem. J. **299**, 165–170
19 Knudsen, J., Færgeman, N. J., Skott, H., Hummel, R., Borsting, C., Rose, T. M., Andersen, J. S., Hojrup, P., Roepstorff, P. and Kristiansen, K. (1994) Yeast acyl-CoA-binding protein: acyl-CoA-binding affinity and effect on intracellular acyl-CoA pool size. Biochem. J. **302**, 479–485

20 Gaigg, B., Neergaard, T. B., Schneiter, R., Hansen, J. K., Færgeman, N. J., Jensen, N. A., Andersen, J. R., Friis, J., Sandhoff, R., Schroder, H. D. and Knudsen, J. (2001) Depletion of acyl-coenzyme A-binding protein affects sphingolipid synthesis and causes vesicle accumulation and membrane defects in *Saccharomyces cerevisiae*. Mol. Biol. Cell **12**, 1147–1160
21 Longtine, M. S., McKenzie, III, A., Demarini, D. J., Shah, N. G., Wach, A., Brachat, A., Philippsen, P. and Pringle, J. R. (1998) Additional modules for versatile and economical PCR-based gene deletion and modification in *Saccharomyces cerevisiae*. Yeast **14**, 953–961
22 Gietz, D., St Jean, A., Woods, R. A. and Schiestl, R. H. (1992) Improved method for high efficiency transformation of intact yeast cells. Nucleic Acids Res. **20**, 1425
23 Veit, M., Laage, R., Dietrich, L., Wang, L. and Ungermann, C. (2001) Vac8p release from the SNARE complex and its palmitoylation are coupled and essential for vacuole fusion. EMBO J. **20**, 3145–3155
24 Haas, A., Conradt, B. and Wickner, W. (1994) G-protein ligands inhibit *in vitro* reactions of vacuole inheritance. J. Cell Biol. **126**, 87–97
25 Ungermann, C., Nichols, B. J., Pelham, H. R. and Wickner, W. (1998) A vacuolar v-t-SNARE complex, the predominant form *in vivo* and on isolated vacuoles, is disassembled and activated for docking and fusion. J. Cell Biol. **140**, 61–69
26 Zinser, E. and Daum, G. (1995) Isolation and biochemical characterization of organelles from the yeast, *Saccharomyces cerevisiae*. Yeast **11**, 493–536
27 Schneiter, R., Brugger, B., Sandhoff, R., Zellnig, G., Leber, A., Lampl, M., Athenstaedt, K., Hrastnik, C., Eder, S., Daum, G. et al. (1999) Electrospray ionization tandem mass spectrometry (ESI-MS/MS) analysis of the lipid molecular species composition of yeast subcellular membranes reveals acyl chain-based sorting/remodeling of distinct molecular species en route to the plasma membrane. J. Cell Biol. **146**, 741–754
28 Vida, T. A. and Emr, S. D. (1995) A new vital stain for visualizing vacuolar membrane dynamics and endocytosis in yeast. J. Cell Biol. **128**, 779–792
29 Kaiser, C. A. and Schekman, R. (1990) Distinct sets of SEC genes govern transport vesicle formation and fusion early in the secretory pathway. Cell **61**, 723–733
30 Mayer, A., Wickner, W. and Haas, A. (1996) Sec18p (NSF)-driven release of Sec17p (α-SNAP) can precede docking and fusion of yeast vacuoles. Cell **85**, 83–94
31 Barlowe, C. (1995) COPII: a membrane coat that forms endoplasmic reticulum-derived vesicles. FEBS Lett. **369**, 93–96
32 Rothman, J. E. and Wieland, F. T. (1996) Protein sorting by transport vesicles. Science **272**, 227–234
33 Burz, D. S., Rivera-Pomar, R., Jackle, H. and Hanes, S. D. (1998) Cooperative DNA-binding by Bicoid provides a mechanism for threshold-dependent gene activation in the *Drosophila* embryo. EMBO J. **17**, 5998–6009
34 Klionsky, D. J., Cueva, R. and Yaver, D. S. (1992) Aminopeptidase I of *Saccharomyces cerevisiae* is localized to the vacuole independent of the secretory pathway. J. Cell Biol. **119**, 287–299
35 Bryant, N. J. and Stevens, T. H. (1998) Vacuole biogenesis in *Saccharomyces cerevisiae*: protein transport pathways to the yeast vacuole. Microbiol. Mol. Biol. Rev. **62**, 230–247
36 Conzelmann, A., Riezman, H., Desponds, C. and Bron, C. (1988) A major 125-kD membrane glycoprotein of *Saccharomyces cerevisiae* is attached to the lipid bilayer through an inositol-containing phospholipid. EMBO J. **7**, 2233–2240
37 Horvath, A., Sutterlin, C., Manning-Krieg, U., Movva, N. R. and Riezman, H. (1994) Ceramide synthesis enhances transport of GPI-anchored proteins to the Golgi apparatus in yeast. EMBO J. **13**, 3687–3695
38 Darsow, T., Rieder, S. E. and Emr, S. D. (1997) A multispecificity syntaxin homologue, Vam3p, essential for autophagic and biosynthetic protein transport to the vacuole. J. Cell Biol. **138**, 517–529
39 Sattler, T. and Mayer, A. (2000) Cell-free reconstitution of microautophagic vacuole invagination and vesicle formation. J. Cell Biol. **151**, 529–538
40 Hearn, J. D., Lester, R. L. and Dickson, R. C. (2003) The uracil transporter Fur4p associates with lipid rafts. J. Biol. Chem. **278**, 3679–3686
41 Cowles, C. R., Odorizzi, G., Payne, G. S. and Emr, S. D. (1997) The AP-3 adaptor complex is essential for cargo-selective transport to the yeast vacuole. Cell **91**, 109–118
42 Nichols, B. J., Ungermann, C., Pelham, H. R., Wickner, W. T. and Haas, A. (1997) Homotypic vacuolar fusion mediated by t- and v-SNAREs. Nature (London) **387**, 199–202
43 Hamamatsu, S., Shibuya, I., Takagi, M. and Ohta, A. (1994) Loss of phosphatidylserine synthesis results in aberrant solute sequestration and vacuolar morphology in *Saccharomyces cerevisiae*. FEBS Lett. **348**, 33–36
44 Kato, M. and Wickner, W. (2001) Ergosterol is required for the Sec18/ATP-dependent priming step of homotypic vacuole fusion. EMBO J. **20**, 4035–4040
45 Schorling, S., Vallee, B., Barz, W. P., Riezman, H. and Oesterhelt, D. (2001) Lag1p and Lac1p are essential for the acyl-CoA-dependent ceramide synthase reaction in *Saccharomyces cerevisiae*. Mol. Biol. Cell **12**, 3417–3427
46 Guillas, I., Kirchman, P. A., Chuard, R., Pfefferli, M., Jiang, J. C., Jazwinski, S. M. and Conzelmann, A. (2001) C26-CoA-dependent ceramide synthesis of *Saccharomyces cerevisiae* is operated by Lag1p and Lac1p. EMBO J. **20**, 2655–2665
47 Chung, J. H., Lester, R. L. and Dickson, R. C. (2003) Sphingolipid requirement for generation of a functional v1 component of the vacuolar ATPase. J. Biol. Chem. **278**, 28872–28881
48 Bagnat, M., Chang, A. and Simons, K. (2001) Plasma membrane proton ATPase Pma1p requires raft association for surface delivery in yeast. Mol. Biol. Cell **12**, 4129–4138
49 Dupre, S. and Haguenauer-Tsapis, R. (2003) Raft partitioning of the yeast uracil permease during trafficking along the endocytic pathway. Traffic **4**, 83–96
50 Kohlwein, S. D., Eder, S., Oh, C. S., Martin, C. E., Gable, K., Bacikova, D. and Dunn, T. (2001) Tsc13p is required for fatty acid elongation and localizes to a novel structure at the nuclear–vacuolar interface in *Saccharomyces cerevisiae*. Mol. Cell Biol. **21**, 109–125
51 Albert, S. and Gallwitz, D. (1999) Two new members of a family of Ypt/Rab GTPase-activating proteins – promiscuity of substrate recognition. J. Biol. Chem. **274**, 33186–33189
52 Munn, A. L. and Riezman, H. (1994) Endocytosis is required for the growth of vacuolar H^+-ATPase-defective yeast: identification of six new END genes. J. Cell Biol. **127**, 373–386

Received 18 December 2003/24 February 2004; accepted 19 March 2004
Published as BJ Immediate Publication 19 March 2004, DOI 10.1042/BJ20031949